J Appl Electrochem (2008) 38:239–244
DOI 10.1007/s10800-007-9431-0

ORIGINAL PAPER

Role of Mo^{6+} during nickel electrodeposition from sulfate solutions

U. S. Mohanty · B. C. Tripathy · P. Singh · S. C. Das · V. N. Misra

Received: 22 August 2005 / Revised: 27 September 2007 / Accepted: 5 October 2007 / Published online: 20 October 2007

Abstract The effect of Mo^{6+} on the current efficiency, deposit quality, surface morphology, crystallographic orientations and polarisation behaviour of the cathode during electrodeposition of nickel from sulfate solutions was investigated. Mo^{6+} did not have a significant effect on current efficiency over the concentration range 2–100 mg dm^{-3}. However; a decrease in current efficiency by a magnitude of more than 20% was seen at 500 mg dm^{-3}. The quality of the nickel deposit with reference to the visual appearance and contamination level varied with varying concentration of Mo^{6+}; this was also reflected in the morphology and crystallographic orientations of the deposits. Addition of Mo^{6+} to the electrolyte introduced two new crystal planes i.e., (220) and (311). Depolarisation of the cathode was noted at lower concentrations of Mo^{6+} (2–40 mg dm^{-3}) whereas polarisation of the cathode was observed at Mo^{6+} concentration >40 mg dm^{-3} .The effect of Mo^{6+} on parameters such as Tafel slope (b), transfer coefficient (α) and exchange current density (i_0) were also determined.

U. S. Mohanty (✉)
Centre for Micro Nano Science and Technology, National Cheng Kung University, Tainan 701, Taiwan, ROC
e-mail: suryaudit@yahoo.com

B. C. Tripathy · S. C. Das · V. N. Misra
Institute of Minerals and Materials Technology (CSIR), Bhubaneswar 751 013, India

S. C. Das
e-mail: sarat.chandradas@gmail.com

B. C. Tripathy
Hydro Metallurgy Division, MINTEK, 200 Hans Stridjom Drive, Randburg 2125, South Africa

P. Singh
Department of Chemistry, Murdoch University, Perth, WA 6150, Australia

Keywords Current efficiency · Deposit morphology · Electrodeposition · Nickel · Polarisation · Molybdenum

1 Introduction

The electrodeposition of nickel has been studied by several investigators with respect to current efficiency (CE), polarisation behaviour and deposit structural characteristics [1–12]. However, scant information [13–17] is available on the effect of cationic impurities on the electrodeposition of nickel from sulfate solutions. Gogia and Das [13] observed that the deposit characteristics and polarisation behaviour were affected strongly in the presence of impurities Mg^{2+}, Mn^{2+}, Al^{3+} and Zn^{2+} but there was no significant change in the CE at very low concentrations during electrodeposition of nickel from acidic sulfate solutions. In a separate study [14] they observed an almost similar effect on nickel deposition process in the presence of low concentrations of cations viz. Co^{2+}, Cu^{2+}, Fe^{2+} and Fe^{3+}. However, higher concentration levels e.g., 1,000 mg dm^{-3} Co^{2+} and 250 mg dm^{-3} Cu^{2+} produced cracked, peeled and black nodular deposits. Holm and O'Keefe [15] studied the effect of varying concentrations of Al^{3+} on the current efficiency and morphology of nickel electrodeposited from acid sulfate electrolyte. They found that Al^{3+} concentrations in the range of 20–100 mg dm^{-3} significantly degraded the nickel-cathode morphology and affected the current efficiency. Higher concentrations of Al^{3+} i.e., 1 to 5 gdm^{-3}, however improved the morphology. Zhou et al. [16] also studied the effect of Al^{3+} and Cr^{3+} on the CE, surface morphology and polarisation behaviour of the cathode during nickel electrowinning from sulfate solutions. They found that CE decreased in the presence of these impurities and the surface morphology, internal stress and polarisation behaviour at the cathode were also affected. Tripathy et al. [17]

studied the effect of metal ions such as Mg^{2+}, Li^{+}, Na^{+} and K^{+} on the CE, deposit morphology, crystallographic orientations and polarisation behaviour of the cathode during electrodeposition of nickel from aqueous sulfate solutions containing boric acid. There was virtually no change in CE in the presence of these metal ions, but there were some modifications of deposit morphology and crystal orientations.

Mohanty et al. [18] studied the effect of Cr^{3+} on the electrodeposition of nickel from acidic sulfate solutions. They observed that a progressive decrease in CE was seen with increasing Cr^{3+} concentration, which showed a maximum decrease of $\sim$10–13% at a concentration of $\sim$100 mg dm^{-3}. Polarisation of the cathode was also seen in the presence of Cr^{3+} in the electrolyte along with a shift in the electroreduction potential of nickel (II) ion towards more negative values. They also made a detailed study on the effect of Cd^{2+} [19] on the CE, deposit characteristics and crystallographic orientations of nickel and the polarisation behaviour of the cathode [20] from sulfate baths of varying compositions. CE and deposit characteristics changed significantly at higher Cd^{2+} concentrations in all the baths whereas highest polarisation of the cathode was observed in the nickel bath containing boric acid.

The present paper reports results of the effect of Mo^{6+} on the CE, deposit quality, surface morphology and crystallographic orientations during electrodeposition of nickel from sulfate solutions. The role of Mo^{6+} on the polarisation behaviour of stainless steel and nickel cathodes was also investigated at 25 °C and the kinetic parameters for the electron transfer process on both the electrodes were determined from the polarisation curves.

2 Experimental

The rectangular electrolytic flow-through cell used in this work was similar to that described previously [21]. The flow cell was made from Perspex and was of dimensions 13.2 × 8 × 6 cm. The cell consisted of cathodic and anodic compartments each of dimensions 9 × 4× 6 cm separated by a microporous Daramic separator. The anolyte and catholyte were circulated into their respective compartments by separate peristaltic pumps (Cole–Parmer Instrument, Australia, model 7553-75) through inlet and outlet ports made from Teflon. The nickel electrolyte containing Ni (60 g dm^{-3}), Na_2SO_4 (12 g dm^{-3}) and H_3BO_3 (12 g dm^{-3}) was prepared from analytical grade reagents (Merck). Dilute sulfuric acid was used to adjust the electrolyte pH. The Mo^{6+} concentration in the baths was achieved by adding aliquots of ammonium phosphomolybdate (Aldrich) stock solution of concentration 10 g dm^{-3}. The Mo^{6+} concentration in the electrolyte was varied from 2 to 500 mg dm^{-3}. All the solutions were prepared from ultrapure Millipore water (Millipore Milli Q system). All the electrodeposition experiments were conducted for 2 h at a current density of 200 A m^{-2} by applying current from a regulated power supply (0–30 V, 5 A, d.c. power supply, Dick Smith Electronics). A precision voltmeter and ammeter were placed in the cell circuit to record the potentials and current. The electrolyte flow rate was maintained at 1.8 dm^3 h^{-1}. A thermostat (Grant Selby's, Australia) was used for maintaining the electrolyte temperature at 60 ± 1 °C. The pH of the electrolyte was maintained at 2.5 using dilute H_2SO_4. Stainless steel and lead antimony (1–5% Sb) were used as cathode and anode, respectively. All the potentials were measured against a saturated calomel electrode (SCE). After electrolysis, the cathode was removed from the cell and thoroughly washed with water and dried. The cathodic current efficiency (CE) was calculated from the weight gained by the cathode. The crystallographic orientations and the surface morphology of the nickel deposits were determined using standard X-ray diffraction and scanning electron microscopy (SEM) as described previously [22]. The experimental set up and procedure followed for polarisation studies were similar to our previous paper [23]. A stainless steel disk electrode of 3 mm diameter (Austenitic grade 316) and platinum wire of 0.5 mm diameter were used as working and auxillary electrodes respectively. A saturated calomel electrode (SCE) was used as the reference electrode and all the potentials were reported as such. The cathode potential was scanned in the potential range 0 to –1000 mV at a scan rate of 10 mV s^{-1} using a PAR (Model 273 A) potentiostat/galvanostat. High purity nitrogen was used to sparge out dissolved oxygen and to maintain an inert atmosphere throughout the polarization studies. From the cathodic polarization curves for nickel deposition the various kinetic parameters were determined using the following equations:

$$\eta = a + b \log I \quad (1)$$

$$b = RT/\alpha nF \quad (2)$$

where η is the overpotential (V), b is the Tafel slope (V $decade^{-1}$), α is the transfer coefficient and I is the current density (mA cm^{-2}). The exchange current densities i_o for nickel deposition were found by extrapolating the Tafel lines to zero overpotential.

3 Results and discussion

3.1 Current efficiency

The CE data for nickel electrodeposition from the nickel sulfate baths in the presence and absence of Mo^{6+} are noted in Table 1. There is a progressive decrease in CE with increasing concentration of Mo^{6+} i.e., the CE decreases

Table 1 Effect of Mo^{6+} on the CE, cathode contamination and crystallographic orientations of nickel electrodeposited from acidic sulfate bath

$[Mo^{6+}]$/mg dm^{-3}	CE (%)	Cathode contamination (%)	Crystallographic orientation of nickel deposits Relative peak intensities (I/I_0) (%)			
			(111)	(200)	(220)	(311)
0	96.0	–	62	100	–	–
2	96.0	0.023	30	100	13	28
10	95.8	0.116	57	90	77	100
20	95.6	0.153	37	100	33	66
40	95.0	0.299	32	100	2	6
100	93.5	0.672	100	59	23	20
500	70.1	3.6	–	–	–	–

from 95.8% at 10 mg dm^{-3} to 70.1% at 500 mg dm^{-3} of Mo^{6+}. This decrease in CE may be attributed to the simultaneous occurrence of one or more side reactions i.e., (1) increased hydrogen evolution at the cathode surface due to low hydrogen overvoltage on molybdenum [24, 25] (2) co-reduction of molybdenum with nickel (3) adsorption of certain molybdenum species on the electrode surface during electroreduction of Ni^{2+}. A drastic fall in CE at higher Mo^{6+} concentrations may be due to a combination of more than one side reaction, which inhibit nickel ion reduction.

3.2 Surface quality

The nickel deposits obtained from the molybdenum free bath are found to be smooth, bright and uniform. Addition of Mo^{6+} up to 10 mg dm^{-3} produced a number of pits on the cathode surface. Further increase in the Mo^{6+} concentration reduced pitting but, at 100 mg dm^{-3}, the deposit becomes cracked and peels off. This may be due to the increase in internal stress developed in the deposit probably as a result of increased entrapment of hydrogen and other foreign species. A black burnt uniformly cracked columnar deposit was formed at 500 mg dm^{-3} of Mo^{6+}. The black colour observed in the nickel deposit may be attributed to the formation of oxides of molybdenum (Mo_2O_3) [26]. The deterioration of the nickel deposit was so high at 500 mg dm^{-3} of Mo^{6+} that further characterisation by SEM and XRD was not possible. From the above studies it can be said that the tolerance limit of Mo^{6+}, based on surface quality of the nickel deposit, is 40 mg dm^{-3}.

The scanning electron micrographs for the nickel deposits obtained in the presence of varying concentration of Mo^{6+} are shown in Fig. 1 and the results on the effect of Mo^{6+} on the crystallographic orientations of the nickel deposits are listed in Table 1. The crystallographic orientations data obtained from XRD are compared with the JCPDS file of nickel [27]. According to the JCPDS data for nickel, the preferred crystal orientation for the (111) (200) (220) and (311) planes follows the order (111) > (200) > (220) > (311). However, addition of Na_2SO_4 and H_3BO_3 to the pure nickel bath changes the preferred crystal orientation order to (200) > (111). The morphology of the nickel deposit obtained from the pure nickel sulfate solution is shown in Fig. 1a. It consists of round edged crystals of varying sizes i.e., 2 to 15 μm. The addition of 2 mg dm^{-3} of Mo^{6+} to the bath produced a morphology consisting of sharp and round edged crystallites spread uniformly over the cathode surface (Fig. 1b). This

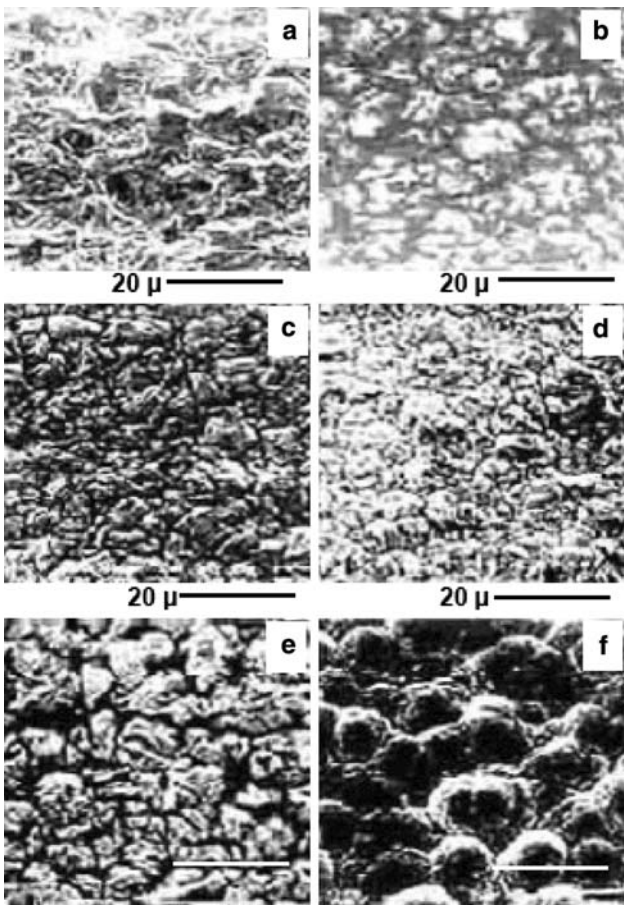

Fig. 1 SE micrographs showing the effect of Mo^{6+} on the surface morphology of the nickel electrodeposits; Key: (**a**) $NiSO_4$ + Na_2SO_4 + H_3BO_3 (**b**) a + 2 mg dm^{-3} Mo^{6+} (**c**) a + 10 mg dm^{-3} Mo^{6+} (**d**) a + 20 mg dm^{-3} Mo^{6+} (**e**) a + 40 mg dm^{-3} Mo^{6+} (**f**) a + 100 mg dm^{-3} Mo^{6+}

results in the formation of two new crystal planes i.e., (220) and (311) and the order of preferred orientation changes to (200) (311) (111) (220). Increasing the Mo^{6+} concentration to 10 mg dm^{-3} results in a more compact deposit (Fig. 1c) where the morphology consists of a bundle of small size crystallites surrounded by larger crystallites (6–8 μm). This is reflected in the change in the order of preferred crystal orientations i.e., (311) (200) (220) (111). Further increase in the Mo^{6+} concentration to 20 mg dm^{-3} produces an entirely different deposit morphology (Fig. 1d), which consists of a group of large crystallites of various shapes, distributed uniformly over the cathode surface and the deposit, looks more compact. This morphology corresponds to a change in the order of preferred crystal orientations as (200) (311) (111) (220). An increase in the Mo^{6+} concentration to 40 mg dm^{-3} increases the size of the crystallites further and results in a morphology consisting of stacks of irregular shaped crystals spread over the cathode surface (Fig. 1e). This is strongly reflected in the significant reduction in the peak intensities of (220) and (311) planes. Finally, a nodular type morphology (Fig. 1f) is seen at 100 mg dm^{-3} of Mo^{6+}; it consists of round shaped coarse crystallites of size varying from 10 to 15 μm. This corresponds to a sudden change in the preferred crystal plane and the order of preferred crystal orientation becomes (111) (200) (220) (311). This preferred crystal orientation obtained at Mo^{6+} concentration of 100 mg dm^{-3} resembles the order of preferred crystal planes for pure nickel obtained from the JCPDS data as mentioned above. The morphology of the deposits could not be characterised beyond 100 mg dm^{-3} because of the deterioration of the nickel deposits.

3.3 Deposit contamination

The nickel electrodeposits obtained at different Mo^{6+} concentrations were analysed for molybdenum contamination. The results are noted in Table 1. All the deposits are found to be contaminated with molybdenum and its content increases with increasing concentration of Mo^{6+} in the nickel electrolyte (0.023% at 2 mg dm^{-3} to 3.6% at 500 mg dm^{-3})

The standard reduction potential of nickel ion, H^+ ion and molybdenum species (Mo^{6+}) in aqueous solution are given below:

$$2H^+ + 2e^- \rightarrow H_2 \quad E^0 = -0.24 \text{ V vs SCE} \tag{3}$$

$$MoO_4^{2-} + 8H^+ + 3e^- \rightarrow Mo^{3+} + 4H_2O \quad E_0 = -0.266 \text{ V vs SCE} \tag{4}$$

$$Mo_3^+ + 3e^- \rightarrow Mo \quad E_0 = -0.442 \text{ V vs SCE} \tag{5}$$

$$Ni^{2+} + 2e^- \rightarrow Ni \quad E_0 = -0.49 \text{ V vs SCE} \tag{6}$$

$$MoO_4^{2-} + 4H_2O + 6e^- \rightarrow Mo + 8OH^- \quad E_0 = -1.29 \text{ V vs SCE} \tag{7}$$

From the standard potential it may be expected that before reduction of Ni^{2+}, reduction of MoO_4^{2-} to Mo through Eqs. 4 and 5 is possible. But it appears improbable for the direct reduction of MoO_4^{2-} to Mo to occur as indicated by Eq. 7. It has been proposed by some authors [28–31] that molybdate (MoO_4^{2-}) is initially electrochemically reduced to molybdenum oxide and subsequently undergoes chemical reduction with atomic hydrogen to form molybdenum in alloys. Thus it is likely that reduction of MoO_4^{2-} to Mo may take place either through Eq. 4 followed by Eq. 5 or by combination of chemical/electrochemical methods as suggested elesewhere [28–31]. Phosphomolybdate species exist in solutions containing both phosphate and molybdate at pH ≤ 7 [32–36]. Since the electrodeposition was carried out at pH < 7 (pH 2.5), it is likely that the electrolyte contains both phosphate and molybdate. Thus the effects shown on nickel electrodeposition in this paper might be mainly due to Mo^{6+}, which is present as MoO_4^{2-}. P, which is present as PO_4^- is unlikely to affect the deposit. However, incorporation of P in the deposit was not verified in the current investigation. Contamination of the nickel deposit in the presence of Mo^{6+} may be attributed to the co-reduction of Mo (VI) to Mo or to the entrapment of oxides [26] formed during the electrodeposition process. The above findings are also strongly reflected in the decrease in CE and deterioration of the surface quality at higher concentration of Mo^{6+}.

3.4 Polarisation behaviour

A typical I–V profile of nickel electrodeposition on nickel and stainless steel substrates is shown in Fig. 2. The Peak 'B' in this figure refers to the reduction of H^+ ions resulting in hydrogen evolution, which occurs prior to nickel deposition. Several authors [37–42], who have studied the fundamental aspects of nickel electrodeposition, have shown that deposition from sulphate solutions is also preceded by hydrogen evolution and starts as soon as hydrogen ion discharge becomes diffusion controlled. The I–V data were used to determine the nucleation overpotential (NOP) and the crossover potential (E_{CO}) by using the following techniques. The potential difference between the points 'C' and 'E' in the polarisation curve (Fig. 2) is a measure of the activation overpotential or the NOP for nickel deposition on the stainless steel substrate (SS). The point 'E' is referred to as the cross-over potential where the cathodic current reaches zero and the potential scan reverses in the

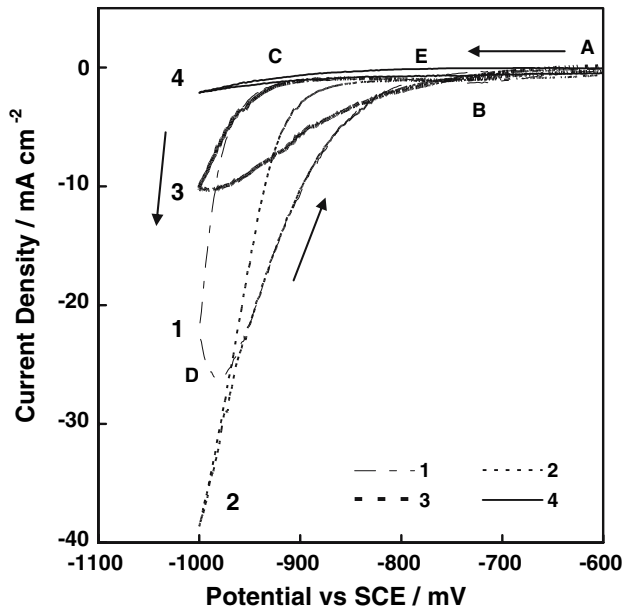

Fig. 2 Cyclic voltammograms showing the effect of varying concentrations of Mo^{6+} during electrodeposition of nickel on a stainless steel substrate; Key: [1] Blank [2] 40 mg dm^{-3} [3] 100 mg dm^{-3} [4] 500 mg dm^{-3}

anodic direction. The cross-overpotential obtained in the present study is around –720 ± 2 mV. The point 'C' in the polarisation curve is referred to as the nucleation potential (E_{Nu}) where nickel starts to nucleate or deposition occurs on the SS substrate. NOP is regarded as an indicator of the extent of polarization of a cathode. High NOP values indicate strong polarisation, whereas low NOP values indicate weak polarisation. For each of the systems the data are noted in Table 2. The NOP value obtained from the molybdenum free bath is –178 mV. However a progressive decease in the NOP value is observed with increase in Mo^{6+} concentration up to 40 mg dm^{-3}. The NOP value suddenly increases with the increase in Mo^{6+} concentration from 40 to 500 mg dm^{-3}. These results indicate that Mo^{6+} ions depolarises the cathode during Ni^{2+} reduction when present at low concentrations (2–40 mg dm^{-3}), nevertheless polarisation of the cathode is observed (Fig. 2) at Mo^{6+} concentration >40 mg dm^{-3}. A similar observation was made by Fukushima et al. [43] during electrodeposition of nickel from ammoniacal tartrate solutions in the presence of MoO_4^{2-}. They suggest that the depolarisation behaviour of the cathode may be due to the adsorption of molybdate ion at the surface which catalyses nickel deposition and the polarisation behaviour of the cathode at higher molybdate concentrations was attributed to the formation of intermediate lower oxides of molybdenum during electrodeposition. This explanation agrees with the present study. These results are also reflected in the variation in CE as reported earlier in Sect. 3.1. The results on the effects of Mo^{6+} on the kinetic parameters b, α and i_0 are given in Table 2. The value 'α' determines the number of electrons involved in the electroreduction process. The exchange current density 'i_o' signifies the rate of reaction occurring at the cathode and anode. Small variations in the *b* values are seen, but it remains around 120 mV except for higher concentrations of Mo^{6+} (100–500 mg dm^{-3}), where it increases. Indicating that the charge transfer is least affected at lower concentrations, but becomes significantly affected at very high concentrations. This may be attributed to the simultaneous side reactions accompanied by electroreduction of Ni^{2+} as discussed earlier. Similar observations have been made by several authors [44–46].

The transfer coefficient (α) remains essentially unaffected in the presence of Mo^{6+} on both the nickel and stainless steel substrates. However the i_0 values change with varying concentration of Mo^{6+} in the nickel electrolyte. For example as noted in Table 2, addition of 2–40 mg dm^{-3} of Mo^{6+} to the electrolyte results in an increase in i_0. However, at higher concentrations of Mo^{6+} (i.e., 40–500 mg dm^{-3}) i_0 decreases for both the nickel and stainless steel substrates. This indicates a higher rate of electron transfer at lower concentrations of Mo^{6+} showing

Table 2 Effect of Mo^{6+} on the kinetic parameters b, α and i_0 for nickel electrodeposition from acidic sulfate bath

[Mo^{6+}]/mg dm^{-3}	NOP/mV	b/mV decade^{-1}		α		i_0/mA cm^{-2}	
		A	B	A	B	A	B
0	–178	–101	–126	0.59	0.47	6.3×10^{-4}	6.8×10^{-3}
2	–172	–122	–120	0.48	0.49	7.0×10^{-4}	7.2×10^{-3}
5	–170	–124	–124	0.47	0.47	7.4×10^{-4}	7.6×10^{-3}
10	–166	–120	–122	0.49	0.48	8.5×10^{-4}	8.2×10^{-3}
20	–162	–110	–125	0.54	0.47	9.0×10^{-4}	8.6×10^{-3}
40	–156	–118	–125	0.50	0.47	9.4×10^{-4}	9.0×10^{-3}
100	–190	–124	–135	0.47	0.44	5.0×10^{-4}	5.2×10^{-3}
500	–208	–135	–139	0.44	0.42	4.4×10^{-4}	4.6×10^{-3}

A = Nickel deposition on stainless steel, B = Nickel deposition over nickel

its catalytic behaviour on nickel deposition. But at higher concentrations the rate of electron transfer decreases due to the formation of oxide [26].

4 Conclusions

It can be concluded that the CE decreases significantly by almost ~20% at 500 mg dm^{-3} of Mo^{6+} in the electrolyte. The tolerance limit of Mo^{6} with regards to surface quality of the nickel deposit is 40 mg dm^{-3}. The molybdenum content in the deposit increases with increasing concentration of Mo^{6+} in the electrolyte (0.023% at 2 mg dm^{-3} to 3.6% at 500 mg dm^{-3}). The peak intensities of various crystal planes and the order of preferred crystal orientation changes with variations in the concentration of Mo^{6+}. This is also reflected in the marked changes in surface morphology. Depolarisation of the cathode occurs at lower concentration of Mo^{6+}; however, polarisation is observed at Mo^{6+} concentration >40 mg dm^{-3}. This is also reflected in the i_0 values.

Acknowledgements USM would first like to thank the CSIR for granting him a research fellowship. The authors thank P. Fallon for assistance with SEM, K. Seymour for XRD and T. B. Issa for general assistance throughout the work. The authors also thank the Director, Regional Research Laboratory Bhubaneswar for his kind permission to publish this paper. Financial support was partly received from the A. J. Parker Cooperative Research Centre for Hydrometallurgy.

References

1. Essin O, Alfimova E (1935) Trans Electrochem Soc 68:417
2. Yuza V, Kopyl I (1940) J Phys Chem 14:1071
3. Salt F (1947) Disc Faraday Soc 1:169
4. Gorbachev A, Yurkevich Y (1954) J Chem Phys 28:1120
5. Fischer H, Seipt M, Morolock G (1955) Z Elektrochem 59:440
6. Yang L (1950) J Electrochem Soc 97:241
7. Clark G, Simonson S (1951) J Electrochem Soc 98:110
8. Wyllie MRF (1948) J Chem Phys 16:52
9. Evans DJ (1958) Trans Faraday Soc 59:1086
10. Cliffe DR, Farr JPG (1964) J Electrochem Soc 111:299
11. Epelboin J, Froment M, Maurin G (1969) Plating 56:1556
12. Reddy AKN (1973) J Electroanal Chem 6:141, 153, 159
13. Gogia SK, Das SC (1988) Met Trans B 19:6
14. Gogia SK, Das SC (1991) J Appl Electrochem 21:64
15. Holm M, Keefe TJO (2000) Met Trans B 31:1203
16. Zhou Z, Holm M, Keefe TJO (1997) In: Proceedings Nickel-Cobalt 97, CIM, Sudbury, Canada
17. Tripathy BC, Das SC, Singh P, Hefter GT, Muir DM (2001) J Appl Electrochem 31:573
18. Mohanty US, Tripathy BC, Singh P, Das SC (2002) Minerals Eng 15:531
19. Mohanty US, Tripathy BC, Singh P, Das SC (2002) J Electroanal Chem 526:63
20. Mohanty US, Tripathy BC, Singh P, Das SC (2004) J Electroanal Chem 566:47
21. Tripathy BC, Singh P, Muir DM (2001) Met Trans B 32:395
22. Mohanty US, Tripathy BC, Singh P, Das SC (2001) J Appl Electrochem 31:579
23. Mohanty US, Tripathy BC, Singh P, Das SC (2001) J Appl Electrochem 31:969
24. Zeng Y, Yao SW, Guo HT (1994) Platinum Surf Fin (Chinese) 16:9
25. Zeng Y, Yao SW, Gao HT (1995) Platinum Surf Fin 82:640
26. Mark HF, Othermer DF, Overberger CG, Seaborg GS (1981) Kirk Othmer encyclopedia of chemical technology, vol. 15, 3rd edn. A Wiley Interscience Publication, p 670
27. Swansou T (1953) Natl Bur Stand (U.S.) Circ 539(1):13
28. Ernst DW, Holt ML (1958) J Electrochem Soc 105:686
29. Chassaing E, Quang KV, Wiart R (1989) J Appl Electrochem 19:839
30. Zeng Y, Yao SW, Guo HT (1995) Act Phys Chem Sin (Chinese) 11:351
31. Zeng Y, Yao SW, Guo HT (1997) Chem J Chem 15:193
32. Souchay P (1963) Polyanions and polycations. Gauthier-Villars, Paris
33. Pope MT (1983) Heteropoly and isopoly oxometallates. Springer-Verlag, Berlin
34. Van Veen JAR, Sudemeiger O, Emeis CA, de Wit HJ (1986) J Chem Soc Dalton Trans 1825
35. Peterson L, Anderson I, Ohman L (1986) Inorg Chem 25:4726
36. Van Veen JAR, Hendris PAJM, Andra RR, Romers EJGM, Wilson AE (1990) J Phys Chem 94:5282
37. Hoare JP (1986) J Electrochem Soc 133:2491
38. Hoare JP (1987) J Electrochem Soc 134:3102
39. Dorsch RK (1969) J Electroanal Chem 21:495
40. Fleischmann M, Reintjes AS (1984) Electrochim Acta 29(1):69
41. Horkans J (1979) J Electrochem Soc 126:1861
42. Pushpavanam M, Balakrishnan K (1996) J Appl Electrochem 26:283
43. Fukushima H, Akiyama T, Nakakoji H, Higashi K (1979) Hyomen Gijutsu 30(11):600
44. Piatti RCV, Arvia AJ, Podesta JJ (1969) Electrochim Acta 14:541
45. Hurlen T (1975) Electrochim Acta 20:499
46. Farndon EE, Walsh FC, Campbell SA (1995) J Appl Electrochem 25:574